Original Article

A cross-sectional study on the correlation of image quality, effective dose, and body composition with thyroid, chest, and abdominal computed tomography scans

Chengxiang Lin[1], Xigang Shen[2], Yajia Gu[2], Zhongwei Qiao[1], Weijun Peng[2]

[1]Department of Radiology, Children's Hospital of Fudan University, National Children's Medical Center, Fudan University, Shanghai, China; [2]Department of Radiology, Fudan University Shanghai Cancer Center, Department of Oncology, Shanghai Medical College, Fudan University, Shanghai, China

Contributions: (I) Conception and design: C Lin, X Shen; (II) Administrative support: C Lin, Z Qiao; (III) Provision of study materials or patients: X Shen, Y Gu, W Peng; (IV) Collection and assembly of data: C Lin, X Shen; (V) Data analysis and interpretation: X Shen, Y Gu, Z Qiao; (VI) Manuscript writing: All authors; (VII) Final approval of manuscript: All authors.

Correspondence to: Xigang Shen, MM; Yajia Gu, MD. Department of Radiology, Fudan University Shanghai Cancer Center, Department of Oncology, Shanghai Medical College, Fudan University, No. 270 Dong'an Road, Xuhui District, Shanghai 200032, China. Email: shen_xg@126.com; cjr.guyajia@vip.163.com; Zhongwei Qiao, MD. Department of Radiology, Children's Hospital of Fudan University, National Children's Medical Center, Fudan University, No. 399 Wanyuan Road, Minhang District, Shanghai 201102, China. Email: qiaozhongwei@163.com.

Background: The rapid increase in the use of radiodiagnostic examinations in China, especially computed tomography (CT) scans, has led to these examinations being the largest artificial source of per capita effective dose (ED). This study conducted a retrospective analysis of the correlation between image quality, ED, and body composition in 540 cases that underwent thyroid, chest, or abdominal CT scans. The aim of this analysis was to evaluate the correlation between the parameters of CT scans and body composition in common positions of CT examination (thyroid, chest, and abdomen) and ultimately inform potential measures for reducing radiation exposure.

Methods: This study included 540 patients admitted to Fudan University Shanghai Cancer Center from January 2015 to December 2019 who underwent both thyroid or chest or abdominal CT scan and body composition examination. Average CT values and standard deviation (SD) values were collected for the homogeneous areas of the thyroid, chest, or abdomen, and the average CT values and SD values of adjacent subcutaneous fat tissue were measured in the same region of interest (ROI). All data were measured three times, and the average was taken to calculate the signal-to-noise ratio (SNR) and contrast-to-noise ratio (CNR) for each area. The dose-length product (DLP) was recorded, and the ED was calculated with the following: formula ED = k × DLP. Dual-energy X-ray was used to determine body composition and obtain indicators such as percentage of spinal and thigh muscle. Pearson correlation coefficient was used to analyze the correlations between body composition indicators, height, weight, body mass index (BMI), and ED.

Results: The correlation coefficients between the SNR of abdominal CT scan and weight, BMI, and body surface area (BSA) were –0.470 (P=0.001), –0.485 (P=0.001), and –0.437 (P=0.002), representing a moderate correlation strength with statistically significant differences. The correlation coefficients between the ED of chest CT scans and weight, BMI, spinal fat percentage, and BSA were 0.488 (P=0.001), 0.473 (P=0.002), 0.422 (P=0.001), and 0.461 (P=0.003), respectively, indicating a moderate correlation strength with statistical differences. There was a weak statistically significant correlation between the SNR, CNR, and ED of the other scans with each physical and body composition index (P=0.023).

Conclusions: There were varying degrees of correlation between CT image quality and ED and physical and body composition indices, which may inform novel solutions for reducing radiation exposure.

Keywords: Effective dose (ED); body composition; signal-to-noise ratio (SNR); contrast-to-noise ratio (CNR)

Submitted Dec 05, 2023. Accepted for publication Apr 12, 2024. Published online May 20, 2024.
doi: 10.21037/qims-23-1731
View this article at: https://dx.doi.org/10.21037/qims-23-1731

Introduction

Considerable effort has been exerted in industry and academia toward reducing radiation exposure during computed tomography (CT) scanning while maintaining image quality and diagnostic accuracy. Over the past decade, developments in CT dose reduction techniques, such as automated tube current modulation (ATCM) and iterative reconstruction, have led to lower radiation doses (1,2), and more recent advancements in CT technology have achieved these reductions without compromising image quality (3). Thus, further research and development may lead to even greater reductions in radiation doses.

Lowering the CT dose may be challenging due to differences in patient volume and weight (4). Larger patients undergoing abdominal pelvis CT scans with ATCM are exposed to significantly higher levels of radiation (5-7). Previous studies have explored the impact of factors such as body weight (6), constitution index (4), patient cross-sectional area (5,7), and patient anterior and posterior diameter (8) on radiation dose during CT scans with ATCM. However, the neck, thorax, and abdominal cavity contain various structures of differing volume and density, influencing these factors. These structures include solid abdominal organs, soft tissue structures such as muscles and adipose tissue, and bone structures such as the thoracic vertebraes, lumbar vertebraes, and pelvis. These components collectively impact patient body mass, body mass index (BMI), and cross-sectional area and thus influence the delivered radiation dose during CT scans with ATCM (9). Although one study found a link between subjective assessment of abdominal fat and radiation exposure (10), a correlation of neck, chest, and abdominal body composition variables with radiation exposure and image quality during CT scans was not found.

Further investigation of these factors may reveal significant differences across individuals with similar weight, cross-sectional area, and constitutional index, the knowledge of which may guide future CT scan dose optimization methods and allow radiologic technologists to specifically optimize examination techniques and ATCM protocols in obese patients. We present this article in accordance with the STROBE reporting checklist (available at https://qims.amegroups.com/article/view/10.21037/qims-23-1731/rc).

Methods

The data set

A retrospective analysis was conducted on a total of 540 patients who underwent CT and body composition examination from January 2015 to December 2019 in Fudan University Shanghai Cancer Center. Among these patients, 105 underwent a thyroid scan, 222 underwent a chest scan, and 213 underwent an abdominal scan. This retrospective study was conducted in accordance with the Declaration of Helsinki (as revised in 2013) and was approved by the institutional medical ethics committee of Fudan University Shanghai Cancer Center (No. 2307278-12). The requirement for individual consent in this retrospective analysis was waived.

The inclusion criteria for patients were as follows: (I) performance of both thyroid, chest, or abdominal CT plain scan or contrast-enhanced scan and body composition examination; and (II) an interval between CT and body composition examinations within 6 months.

Patients with incompatible scanning methods, poor quality of the images that prevented further analysis, and those with contraindications to contrast agents were excluded.

The method of evaluation

CT examinations were performed using the Sensation 40 or Sensation 64 multidetector spiral CT scanner (Siemens Healthineers, Erlangen, Germany). The imaging parameters were a 5 mm slice thickness, 120 kV, and automatic tube current modulation (mAs). Nonionic contrast agents were used, with injection rates set between 1.5 and 3.0 mL/s depending on the individual patient.

Body composition examination

Body composition examination was performed using a Lunar iDXA (GE HealthCare, Chicago, IL, USA). Before

imaging, the patient's height and weight were measured, and menopausal women were asked about their age at menopause. During imaging, the patient was required to remove heavy and unnecessary clothing and not to wear any metallic or other high-density objects such as buttons, keys, coins, zippers, or underwear. The patient lay flat on the examination table, and the dual-energy X-ray absorptiometry (DXA) standard mode was used for scanning. In completing the scan, the scanning arm was moved from the head side to the foot side. Routine images included a supine spine image covering a range from the L1 to L4 Lumbar vertebrae and a left hip image comprising the pubic symphysis, femoral head, femoral neck, and greater trochanter. After the two images were obtained, the system software automatically processed the data and calculated the results.

CT technical data analysis

Signal-to-noise ratio (SNR) and contrast-to-noise ratio (CNR)

The thyroid scan range extended from the external auditory meatus to the bifurcation of the tracheal prominence. Circular regions of interest (ROIs) were manually delineated with a size of 50±2 mm^2. The CT value and standard deviation (SD) value were measured in the homogeneous area of the thyroid. The CT value and SD value of the adjacent subcutaneous fatty tissue were measured in the same ROIs. The chest scan range extended from the T1 to L1 vertebrae. Circular ROIs with a size of 100±5 mm^2 were manually delineated, with the areas of blood vessels, bronchi, and lesions being avoided, and the CT value and SD value were measured. The CT value and SD value of the adjacent subcutaneous fatty tissue were measured in the same ROIs. The abdominal scan range extended from the diaphragm to the iliac crest. Circular ROIs with a size of 100±5 mm^2 were manually delineated, preferably at the right hepatic portal vein branch of the liver, with the areas of the liver vessels and lesions being avoided, and the CT value and SD value of the liver parenchyma were measured. The CT value and SD value of the adjacent subcutaneous fatty tissue were measured in the same ROIs. The following values were each measured three times: CT value of tissue (TCTv; TCTv1 + TCTv2 + TCTv3), CT value of fat (FCTv; FCTv1, FCTv2, FCTv3), SD value of tissue (TSDv; TSDv1, TSDv2, TSDv3), and SD value of fat (FSDv; FSDv1, FSDv2, FSDv3). The mean values were calculated. The SNR of each region was calculated as follows: SNR = mean TCTv/mean TSDv. Meanwhile, the CNR of each region was calculated as follows: CNR = (mean TCTv – mean FCTv)/mean FSDv (11). The volume computed tomography dose index (CTDIvoI) and dose-length product (DLP) were simultaneously measured.

The thyroid scan included a plain scan and contrast-enhanced scan. A standard soft-tissue window for the neck region were used, and the ROIs were selected in a homogeneous area of the enhanced sequence with a slice thickness of 5 mm for measurement, with the areas of blood vessels and lesions being avoided. Chest scans were performed as a plain scan with a standard lung and mediastinal window, and ROIs were selected in the lung window sequence with a slice thickness of 5 mm for measurement, with the areas of blood vessels, bronchi, and lesions being avoided. The abdominal scan included a plain scan and contrast-enhanced scan. A standard soft-tissue window for the abdominal region was used, and ROIs were selected in a homogeneous area of the arterial phase in the enhanced sequence with a slice thickness of 5 mm for measurement, with the areas of liver vessels and lesions being avoided.

Effective dose (ED)

The CTDIvol and DLP were recorded, and the ED was calculated as follows: ED = k × DLP. The value of k was 0.0054 mSv/(mGy·cm) for the neck (thyroid), 0.0170 mSv/(mGy·cm) for the chest (lung), and 0.0150 mSv/(mGy·cm) for the abdomen (liver) (12). The k values for the neck, chest, and abdomen were 0.0054, 0.017, and 0.015, respectively.

Body composition

Body composition measurements included patient height, weight, BMI, body surface area (BSA), percentage of spine and thigh muscle, and percentage of spine and thigh fat. The BSA was calculated as follows: BSA (m^2) = 0.0061 × height (cm) + 0.0128 × weight (kg) – 0.1529 (13).

Statistical analysis

Statistical analysis was performed via SPSS 21.0 software (IBM Corp., Armonk, NY, USA). One way analysis of variance (ANOVA) was used to analyze the differences in body composition values, height, weight, and BMI among thyroid, chest, and abdominal CT scans. Significant differences were selected for multivariate logistic regression

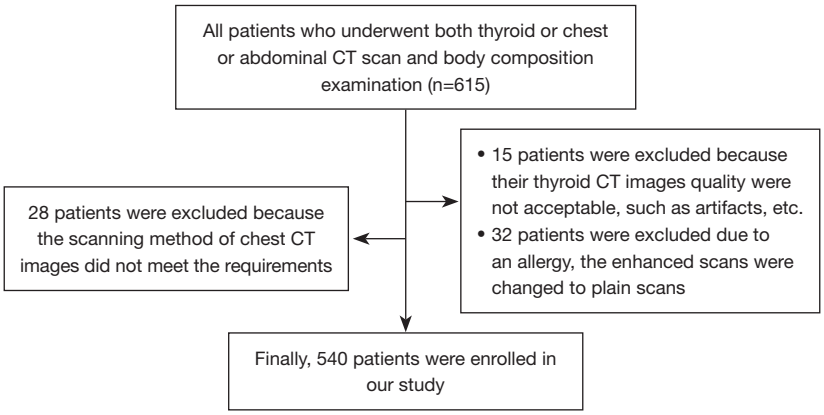

Figure 1 Flowchart showing the patient selection process. CT, computed tomography.

analysis to analyze the causal relationship between variables, as after testing, the data conformed to a normal distribution. Pearson correlation coefficient was used to analyze the correlations between body composition data, height, weight, BMI, and ED. The common range values of correlation strength and their corresponding absolute values were defined as follows: 0.8–1.0, very strong correlation; 0.6–0.8, strong correlation; 0.4–0.6, moderate correlation; 0.2–0.4, weak correlation; and 0.0–0.2, very weak correlation or no correlation. A one-sided P value <0.05 was considered statistically significant (14).

Results

This study examined 615 patients who underwent both a thyroid, chest, or abdominal CT scan and a body composition examination. Of these, 15 patients were excluded because their thyroid CT images quality were not acceptable due to, for example, the presence of artifacts; 28 patients were excluded because the scanning method of chest CT images did not meet the requirements; and 32 patients were excluded due to allergy, with the enhanced scans being changed to plain scans. Ultimately, 540 patients were enrolled in our study. A flow diagram of the participant selection process is presented in *Figure 1*.

Patient information

Among the patients, there were 527 females and 13 males, with ages ranging from 25 to 82 years. The mean age for patients with thyroid, chest, and abdominal CT scans was 52.49±11.54, 56.87±10.80, and 57.39±10.33 years, respectively (*Table 1*).

Relationship between signal-to-noise of thyroid, chest, and abdominal CT and physical parameters and body composition index

The SNR of abdominal CT scan showed a moderate correlation with weight, BMI, and BSA, with correlation coefficients of –0.470, –0.485, and –0.437, respectively, with P values of 0.001, 0.001, and 0.002, respectively, indicating a statistically significant difference. The SNR of thyroid and chest CT scans showed a weak correlation but statistically significant difference with physical parameters and body composition index (P=0.023) (see *Table 2* and *Figures 2-4* for details).

Relationship between CNR of thyroid, chest, and abdominal CT and physical parameters and body composition index

The CNR of thyroid, chest, and abdominal CT scans showed a weak correlation with physical parameters and body composition index (P=0.023) (see *Table 2* and *Figures 2-4* for details).

Relationship between ED of thyroid, chest, and abdominal CT and physical parameters and body composition index

The ED of the chest CT scan showed a moderate correlation with weight, BMI, spine fat percentage, and BSA, with correlation coefficients of 0.488, 0.473, 0.422, and 0.461, respectively, with P values of 0.001, 0.002, 0.001, and 0.0031, respectively, indicating a statistically significant difference. The ED of thyroid and abdominal CT scans showed a weak correlation with physical parameters and body composition index (P=0.023) (see *Table 2* and

Table 1 Basic information of 540 cases

Characteristic	Chest	Abdomen	Thyroid
Gender (F/M)	217/5	206/7	104/1
Age (years)	56.87±10.80	57.39±10.33	52.49±11.54
Height (cm)	160 (157–163)	160 (157–164)	160 (157–163)
Weight (kg)	59.89±9.08	59.51±9.33	59.71±9.72
BMI (kg/m^2)	23.45±3.11	23.28±3.19	23.33±3.46
Thigh fat percentage	27.15 (23.72–30.17)	27.0 (23.7–30.1)	27.0 (24.0–30.0)
Thigh muscle percentage	72.85 (69.73–76.27)	73.0 (69.9–76.3)	73.0 (70.0–76.0)
Spine fat percentage	34.45 (27.05–38.93)	33.5 (25.7–38.7)	31.4 (26.7–39.0)
Spine muscle percentage	65.55 (61.08–72.95)	66.5 (61.3–74.3)	68.6 (61.0–73.3)
BSA	1.59±0.14	1.58±0.14	1.59±0.14

Age, weight, and BMI are described as the mean ± SD. Height, thigh fat, thigh muscle, spine fat, and spine muscle are described as the median (interquartile range). Gender is described as the statistical count. F, female; M, male; BMI, body mass index; BSA, body surface area; SD, standard deviation.

Table 2 Correlation coefficients between CT scan parameters (SNR, CNR, and ED) and body composition in common positions of CT examination (thyroid, chest, and abdomen) in 540 cases

Index	SNR			CNR			ED		
	Abdomen (n=213)	Chest (n=222)	Thyroid (n=105)	Abdomen (n=213)	Chest (n=222)	Thyroid (n=105)	Abdomen (n=213)	Chest (n=222)	Thyroid (n=105)
Height	–0.127	–0.108	–0.039	–0.169*	–0.125	–0.145	0.087	0.175**	0.016
Weight	–0.470**	0.071	–0.215*	–0.028	–0.09	–0.022	0.299**	0.488**	0.262**
BMI	–0.485**	0.146*	–0.218*	0.071	–0.04	0.031	0.304**	0.473**	0.271**
Thigh fat percentage	–0.208**	0.052	–0.057	0.268**	–0.183**	0.117	–0.023	0.259**	0.258**
Thigh muscle percentage	0.208**	0.002	0.057	–0.268**	0.210**	–0.117	0.023	–0.206**	–0.258**
Spine fat percentage	–0.367**	0.043	–0.287**	0.277**	–0.239**	0.194*	0.223**	0.422**	0.184
Spine muscle percentage	0.367**	–0.043	0.287**	–0.278**	0.239**	–0.194*	–0.223**	–0.422**	–0.184
BSA	–0.437**	0.034	–0.201*	–0.065	–0.107	–0.051	0.279**	0.461**	0.238*

**, P<0.01; *, P<0.05. Pearson correlation coefficient was used to analyze the correlations between body composition data, height, weight, BMI, and ED. CT, computed tomography; SNR, signal-to-noise ratio; CNR, contrast-to-noise ratio; ED, effective dose; BMI, body mass index; BSA, body surface area.

Figures 2-4 for details).

Discussion

Our study explored the correlation between ED and body composition in common CT examination positions (thyroid, chest, abdomen). The results showed a moderate correlation between SNR of abdominal CT scan and body composition indices, with the P values all being <0.01 indicating statistical differences. The CNR of the thyroid, chest, and abdominal CT scans were weakly correlated with body composition indices (all P values <0.05). The ED of chest CT scan showed a moderate correlation with body composition indices, with the P values all being <0.01 indicating statistical differences. The ED of thyroid and abdominal CT scans were weakly correlated with various

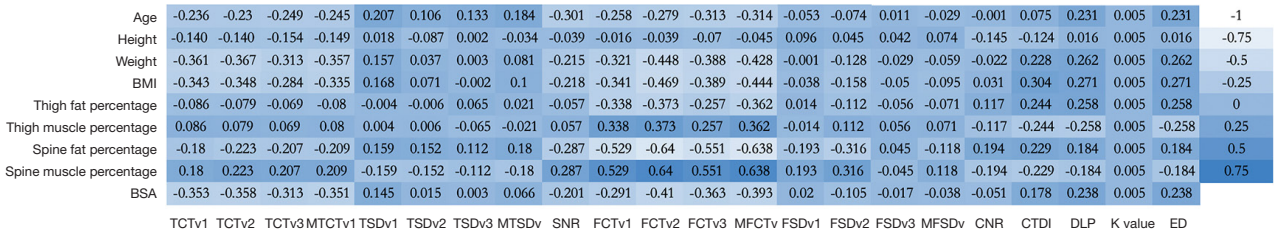

Figure 2 Relationship between the CNR, SNR, and ED of thyroid CT scans and physical parameters and body composition index. BMI, body mass index; BSA, body surface area; TCTv, CT value of tissue; MTCTv, mean tissue CT value; TSDv, SD value of tissue; MTSDv, mean tissue SD value; SNR, signal-to-noise ratio; FCTv, CT value of fat; MFCTv, mean fat CT value; FSDv, SD value of fat; MFSDv, mean fat SD value; SD, standard deviation; CNR, contrast-to-noise ratio; CTDI, CT dose index; DLP, dose-length product; ED, effective dose; CT, computed tomography.

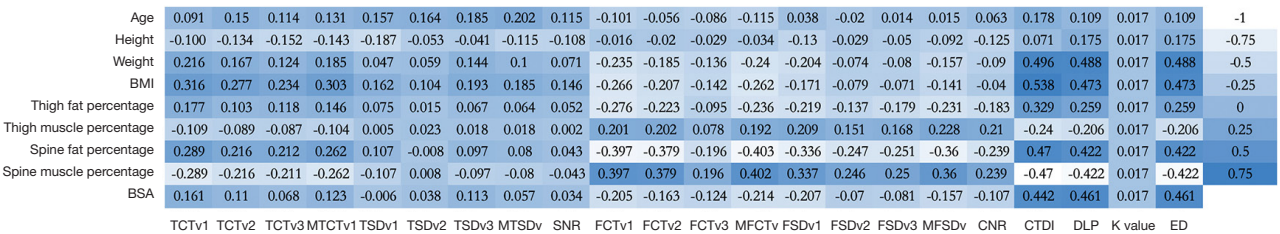

Figure 3 Relationship between the CNR, SNR, and ED of chest CT and physical parameters and body composition index. BMI, body mass index; BSA, body surface area; TCTv, CT value of tissue; MTCTv, mean tissue CT value; TSDv, SD value of tissue; MTSDv, mean tissue SD value; SNR, signal-to-noise ratio; FCTv, CT value of fat; MFCTv, mean fat CT value; FSDv, SD value of fat; MFSDv, mean fat SD value; SD, standard deviation; CNR, contrast-to-noise ratio; CTDI, CT dose index; DLP, dose-length product; ED, effective dose; CT, computed tomography.

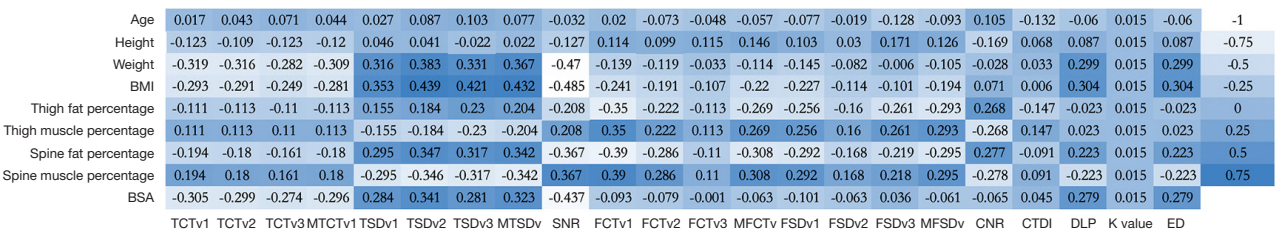

Figure 4 Relationship between the CNR, SNR, and ED of abdominal CT and physical parameters and body composition index. BMI, body mass index; BSA, body surface area; TCTv, CT value of tissue; MTCTv, mean tissue CT value; TSDv, SD value of tissue; MTSDv, mean tissue SD value; SNR, signal-to-noise ratio; FCTv, CT value of fat; MFCTv, mean fat CT value; FSDv, SD value of fat; MFSDv, mean fat SD value; SD, standard deviation; CNR, contrast-to-noise ratio; CTDI, CT dose index; DLP, dose-length product; ED, effective dose; CT, computed tomography.

body measurements and indices (all P values <0.05). It can be surmised that there is a potential association between ED and ED of thyroid, chest, and abdominal CT scans, and further research is needed to clarify the related mechanisms and relationships. With the advancement of medical imaging technology and the increasing need for medical diagnosis and treatment, the application of CT scan in disease diagnosis, differential diagnosis, and follow-up has become more prevalent. Medical irradiation has become the largest source of artificial ionizing radiation, and the degree to which humans are exposed to it is continuously increasing (15-17). CT is currently the most important source of

radiation exposure in diagnostic radiology, contributing the most to medical ED. Radiation-induced deterministic and stochastic effects have been reported as being radiation damage caused by CT radiation (3). Therefore, the issue of the relative benefits of ED has garnered increased attention and has become a focal point in medical research.

Currently, weight and BMI are considered the most common parameters related to CT radiation exposure (4-8). In 2015, the World Health Organization classified a BMI of 18.5–24.9 kg/m^2 as normal for adults, a BMI of ≥25.0 kg/m^2 as obese status, and a BMI of <18.5 kg/m^2 as underweight status. Some researchers in China have studied the reduction of ED based on BMI (10,11), but the relationship between BMI and ED has not been elucidated. Saade *et al.* (15) divided individuals into four groups based on different weights (≤60, 60–80, 81–100, and ≥101 kg) and studied the impact of weight on ED, finding a relationship between weight and ED. Due to the lower average body weight of the population in China compared to Western countries (16), Chen *et al.* (17) divided their study population into two groups based on a weight of 60, ≤60, and >60 kg and used different scanning parameters for each group. They also found that weight can affect CT ED. It is widely known that the energy of X-ray photons depends on the tube voltage. In turn, the tube voltage determines the penetration power of X-rays, and there exists an exponential mathematical relationship between tube voltage and radiation dose. Its variation can significantly impact radiation dose (18); however, the reduction of radiation dose due to tube voltage is limited. A too-low X-ray photon energy can result in poor penetration, especially for patients with a BMI, potentially increasing image noise and hampering diagnostic accuracy (19). The tube current determines the intensity of X-rays and is directly proportional to radiation dose (20). However, lowering the tube current also has its limitations. When the tube current is too low, image noise increases, requiring larger tube currents to reduce image noise to an acceptable level, particularly for patients with a high BMI. Therefore, judicious adjustment of both tube voltage and tube current is an effective method for reducing the radiation dose (21,22).

Although the increased image noise associated with the use of lower tube voltage can be partially compensated by the elevated T values to some extent, this compensation is not always complete. Our study demonstrated a moderate negative correlation between weight, BMI and BSA, and the SNR in abdominal CT, with correlation coefficients of –0.470, –0.485, and –0.437, respectively. This could be attributable to the fact that individuals with a higher BMI tend to have visceral fat mainly distributed in the abdomen. Consequently, not all populations are suitable for a lower tube voltage, and this is particularly crucial for abdominally CT-scanned patients with a higher BMI. Using a lower tube voltage in individuals with higher BMI can lead to excessive image noise, reducing the sharpness of vessel edges and making it challenging to detect small noncalcified plaques. This, in turn, results in a reduced diagnostic accuracy. In such cases, the increased image noise can be mitigated by using a higher tube current (23).

Automatic tube potential selection with tube current modulation (APSCM) technique can be used to automatically determine the patient's body size based on localizer images. It then calculates the baseline and variation curve of the required tube current under different tube voltages according to preset image quality levels and application purposes. Moreover, it calculates the CTDIvol (10,11). The use of APSCM technique during CT examinations significantly reduces the radiation dose compared to BMI-based tube voltage adjustment while maintaining good subjective image quality (12). However, the unsuitable selection of lower tube voltage that leads to increased image noise is more apparent in obese patients, partially compromising the objective image quality. Previous studies have mainly focused on low-dose techniques, but whether consistent image quality can be achieved with low-dose techniques for different patients is also worth exploring.

Several studies have attempted to use BMI as a key parameter for current modulation. For instance, in coronary CT imaging using APSCM, better image quality can be obtained, but image noise, SNR, and CNR still correlate with patient BMI (24). Adjusting tube voltage based on BMI combined with ATCM shows no significant correlation between image noise and patient BMI, resulting in more consistent image quality compared to APSCM technology. This suggests that BMI alone may not be sufficient as a key parameter for personalized current modulation based on body size. Our study also attempted to examine the relationship between weight, BMI, body composition, ED, and image quality to support the more personalized development of APSCM technology.

Body composition analyzers are instruments used to assess the body composition index through directly measuring or using statistical methods. They can measure various health indices of patients, such as weight, basal metabolic rate, bone mass, muscle mass, visceral fat

level, etc., and infer the patient's body age, body fat percentage, and degree of obesity (25-27). Additionally, body composition analyzers can provide precise health indices for the upper, lower, left, and right limbs of patients, effectively indicating various health indicators. In clinical diagnosis and treatment, patients often experience clinical manifestations such as anorexia, weight loss, and decreased muscle function due to diseases and other reasons, resulting in changes in their body composition (28-30). With the increasing demand for health awareness, the importance of health has been recognized, and body composition analyzers have been widely applied. Based on professional analysis using body composition analyzers, healthcare professionals can accurately assess changes in patients' body composition, which helps them make medical diagnostic judgments, manage chronic diseases, and formulate nutritional management plans (31). Currently, reducing ED during CT scanning while maintaining image quality and diagnostic accuracy is a significant focus of academic and industrial research. Thus far, CT dose-reduction technologies, including ATCM and iterative reconstruction, have reduced CT dose levels by approximately 70–75% compared to a decade ago (32). With ongoing research and development, further dose reduction is possible, and the latest advances in CT technology have enabled significant dose reductions without sacrificing image quality. However, the differences in patient size and weight pose challenges to reducing CT ED. It is well known that patients with larger body sizes are exposed to significantly higher levels of ionizing radiation during abdominal and pelvic CT scans when ATCM is used (4-7). Previous studies have examined the influence of variables such as weight (6), BMI (4), patient cross-sectional area (5,7), and patient anterior-posterior (AP) diameter (8) on the dose delivered during ATCM abdominal and pelvic CT examinations. However, the abdominal region accommodates many structures of different volumes and densities, which can influence these indices. These components include solid abdominal organs, soft tissue structures such as abdominal muscle tissue and adipose tissue, and bone structures such as the lumbar vertebrae and pelvis. These structures contribute to the patient's weight, BMI, and cross-sectional area and may individually contribute to the dose during abdominal and pelvic CT scans. A previous study reported a correlation between subjective grading of abdominal fat and ED (33), and our previous study on the correlation between breast X-ray imaging and body composition also found a high correlation between body composition and dose (34).

Limitations

Although our sample size was sufficiently large, the gender distribution of the participants in our study was uneven. This could potentially restrict the generalizability of our findings, and further research is needed to compare the differences between genders.

Conclusions

There is a relationship between the ED of CT in major body parts and body composition indices. After further data validation, these indices may be expected to become an important parameter for reducing ED in CT scanning schemes.

Acknowledgments

Funding: None.

Footnote

Reporting Checklist: The authors have completed the STROBE reporting checklist. Available at https://qims.amegroups.com/article/view/10.21037/qims-23-1731/rc

Conflicts of Intertest: All authors have completed the ICMJE uniform disclosure form (available at https://qims.amegroups.com/article/view/10.21037/qims-23-1731/coif). The authors have no conflicts of interest to declare.

Ethical Statement: The authors are accountable for all aspects of the work in ensuring that questions related to the accuracy or integrity of any part of the work are appropriately investigated and resolved. This retrospective study was conducted in accordance with the Declaration of Helsinki (as revised in 2013) and was approved by the institutional medical ethics committee of Fudan University Shanghai Cancer Center (No. 2307278-12). The requirement for individual consent in this retrospective analysis was waived.

References

1. Amis ES Jr. CT radiation dose: trending in the right direction. Radiology 2011;261:5-8.
2. Marcus RP, Koerner E, Aydin RC, Zinsser D, Finke T, Cyron CJ, Bamberg F, Nikolaou K, Notohamiprodjo M. The evolution of radiation dose over time: Measurement of a patient cohort undergoing whole-body examinations on three computer tomography generations. Eur J Radiol 2017;86:63-9.
3. Scholtz JE, Wichmann JL, Hüsers K, Beeres M, Nour-Eldin NE, Frellesen C, Vogl TJ, Lehnert T. Automated tube voltage adaptation in combination with advanced modeled iterative reconstruction in thoracoabdominal third-generation 192-slice dual-source computed tomography: effects on image quality and radiation dose. Acad Radiol 2015;22:1081-7.
4. Mulkens TH, Bellinck P, Baeyaert M, Ghysen D, Van Dijck X, Mussen E, Venstermans C, Termote JL. Use of an automatic exposure control mechanism for dose optimization in multi-detector row CT examinations: clinical evaluation. Radiology 2005;237:213-23.
5. Schindera ST, Nelson RC, Toth TL, Nguyen GT, Toncheva GI, DeLong DM, Yoshizumi TT. Effect of patient size on radiation dose for abdominal MDCT with automatic tube current modulation: phantom study. AJR Am J Roentgenol 2008;190:W100-5.
6. Israel GM, Cicchiello L, Brink J, Huda W. Patient size and radiation exposure in thoracic, pelvic, and abdominal CT examinations performed with automatic exposure control. AJR Am J Roentgenol 2010;195:1342-6.
7. Meeson S, Alvey CM, Golding SJ. The in vivo relationship between cross-sectional area and CT dose index in abdominal multidetector CT with automatic exposure control. J Radiol Prot 2010;30:139-47.
8. Zarb F, Rainford L, McEntee MF. AP diameter shows the strongest correlation with CTDI and DLP in abdominal and chest CT. Radiat Prot Dosimetry 2010;140:266-73.
9. McLaughlin PD, Chawke L, Twomey M, Murphy KP, O'Neill SB, McWilliams SR, James K, Kavanagh RG, Sullivan C, Chan FE, Moore N, O'Connor OJ, Eustace JA, Maher MM. Body composition determinants of radiation dose during abdominopelvic CT. Insights Imaging 2018;9:9-16.
10. Chan VO, McDermott S, Buckley O, Allen S, Casey M, O'Laoide R, Torreggiani WC. The relationship of body mass index and abdominal fat on the radiation dose received during routine computed tomographic imaging of the abdomen and pelvis. Can Assoc Radiol J 2012;63:260-6.
11. Gonzalez-Guindalini FD, Ferreira Botelho MP, Töre HG, Ahn RW, Gordon LI, Yaghmai V. MDCT of chest, abdomen, and pelvis using attenuation-based automated tube voltage selection in combination with iterative reconstruction: an intrapatient study of radiation dose and image quality. AJR Am J Roentgenol 2013;201:1075-82.
12. European Communities. European Guidelines on Quality Criteria for Computed Tomography. Report Eur 1999;16262.
13. Wu Q, Zhou Y, Fan X, Ma H, Gu W, Sun F. Evaluation of nine formulas for estimating the body surface area of children with hematological malignancies. Front Pediatr 2022;10:989049.
14. Rosenkrantz AB, Lim RP, Haghighi M, Somberg MB, Babb JS, Taneja SS. Comparison of interreader reproducibility of the prostate imaging reporting and data system and likert scales for evaluation of multiparametric prostate MRI. AJR Am J Roentgenol 2013;201:W612-8.
15. Saade C, Ammous A, Abi-Ghanem AS, Giesel F, Asmar K. Body Weight-Based Protocols During Whole Body FDG PET/CT Significantly Reduces Radiation Dose without Compromising Image Quality:Findings in a Large Cohort Study. Acad Radiol 2019;26:658-63.
16. Fang C, Liang Y. Social disparities in body mass index (BMI) trajectories among Chinese adults in 1991-2011. Int J Equity Health 2017;16:146.
17. Chen Z, Chen Z, Zhing Q, Xiao H, Xu S, Fu L, Tao C. Study on CT radiation dose and image quality of PET/CT based on optimized CT scanning parameters according to the weight. China Medical Equipment 2019;34:25-7,34.
18. Layritz C, Muschiol G, Flohr T, Bietau C, Marwan M, Schuhbaeck A, Schmid J, Ropers D, Achenbach S, Pflederer T. Automated attenuation-based selection of tube voltage and tube current for coronary CT angiography: reduction of radiation exposure versus a BMI-based strategy with an expert investigator. J Cardiovasc Comput Tomogr 2013;7:303-10.
19. Park YJ, Kim YJ, Lee JW, Kim HY, Hong YJ, Lee HJ, Hur J, Nam JE, Choi BW. Automatic Tube Potential Selection with Tube Current Modulation (APSCM) in coronary CT angiography: Comparison of image quality and radiation dose with conventional body mass index-based protocol. J Cardiovasc Comput Tomogr 2012;6:184-90.

20. Deetjen A, Möllmann S, Conradi G, Rolf A, Schmermund A, Hamm CW, Dill T. Use of automatic exposure control in multislice computed tomography of the coronaries: comparison of 16-slice and 64-slice scanner data with conventional coronary angiography. Heart 2007;93:1040-3.
21. Rizzo S, Kalra M, Schmidt B, Dalal T, Suess C, Flohr T, Blake M, Saini S. Comparison of angular and combined automatic tube current modulation techniques with constant tube current CT of the abdomen and pelvis. AJR Am J Roentgenol 2006;186:673-9.
22. Gudjónsdóttir J, Ween B, Olsen DR. Optimal use of AEC in CT: a literature review. Radiol Technol 2010;81:309-17.
23. Gordic S, Desbiolles L, Sedlmair M, Manka R, Plass A, Schmidt B, Husarik DB, Maisano F, Wildermuth S, Alkadhi H, Leschka S. Optimizing radiation dose by using advanced modelled iterative reconstruction in high-pitch coronary CT angiography. Eur Radiol 2016;26:459-68.
24. Li H, Zhang Z, Li F, Ge Y, Liang R, Zhang Z, Yanf F, Li D. Quantitative measurement of chest wall components: a potential patient-specific replacement for BMI to predict image quality parameters in coronary CT angiography. Chin J Acad Radiol 2020;3:143-51.
25. Kim SB, Shin TM, Lee YH. Development and evaluation of a bio-ion measurement system on acupoints for meridian diagnosis. J Acupunct Meridian Stud 2013;6:110-8.
26. Franz D, Karampinos DC, Rummeny EJ, Souvatzoglou M, Beer AJ, Nekolla SG, Schwaiger M, Eiber M. Discrimination Between Brown and White Adipose Tissue Using a 2-Point Dixon Water-Fat Separation Method in Simultaneous PET/MRI. J Nucl Med 2015;56:1742-7.
27. Bertrandt J, Szarska E, Łakomy R, Lepionka T, Anyżewska A, Lorenz K, Maculewicz E. An Attempt to Utilize the Body Composition Analyzer and the Functional Movement Screen (FMS) Test to Determine Injury Risk in Soldiers. Mil Med 2020;185:e1128-33.
28. Zhao L. Effects of nutritional interventions on body composition and blood sugar in newly diagnosed type 2 diabetic patients with overweight and obesity. China Health Vision 2019;24:127.
29. Ochoa-Repáraz J, Kasper LH. The Second Brain: Is the Gut Microbiota a Link Between Obesity and Central Nervous System Disorders? Curr Obes Rep 2016;5:51-64.
30. Meredith-Jones KA, Williams SM, Taylor RW. Bioelectrical impedance as a measure of change in body composition in young children. Pediatr Obes 2015;10:252-9.
31. Ormseth MJ, Lipson A, Alexopoulos N, Hartlage GR, Oeser AM, Bian A, Gebretsadik T, Shintani A, Raggi P, Stein CM. Association of epicardial adipose tissue with cardiometabolic risk and metabolic syndrome in patients with rheumatoid arthritis. Arthritis Care Res (Hoboken) 2013;65:1410-5.
32. Marcus RP, Koerner E, Aydin RC, Zinsser D, Finke T, Cyron CJ, Bamberg F, Nikolaou K, Notohamiprodjo M. The evolution of radiation dose over time: Measurement of a patient cohort undergoing whole-body examinations on three computer tomography generations. Eur J Radiol 2017;86:63-9.
33. Wang Y, Han H, Shi Y, Ye H, Yao N, Yu J. Effect of abdominal adipose content on spine phantom bone mineral density measured by low-mA quantitative CT. Chinese Journal of Osteoporosis 2023;29:173-8.
34. Shen X, Gu Y, Zheng X, Chen C, Li R, Xiao Q, Zhou L, Peng W. The correlation study among mammographic radiation dose, breast density and body composition in breast cancer. China Oncology 2018;28:755-61.

Cite this article as: Lin C, Shen X, Gu Y, Qiao Z, Peng W. A cross-sectional study on the correlation of image quality, effective dose, and body composition with thyroid, chest, and abdominal computed tomography scans. Quant Imaging Med Surg 2024;14(6):4031-4040. doi: 10.21037/qims-23-1731

